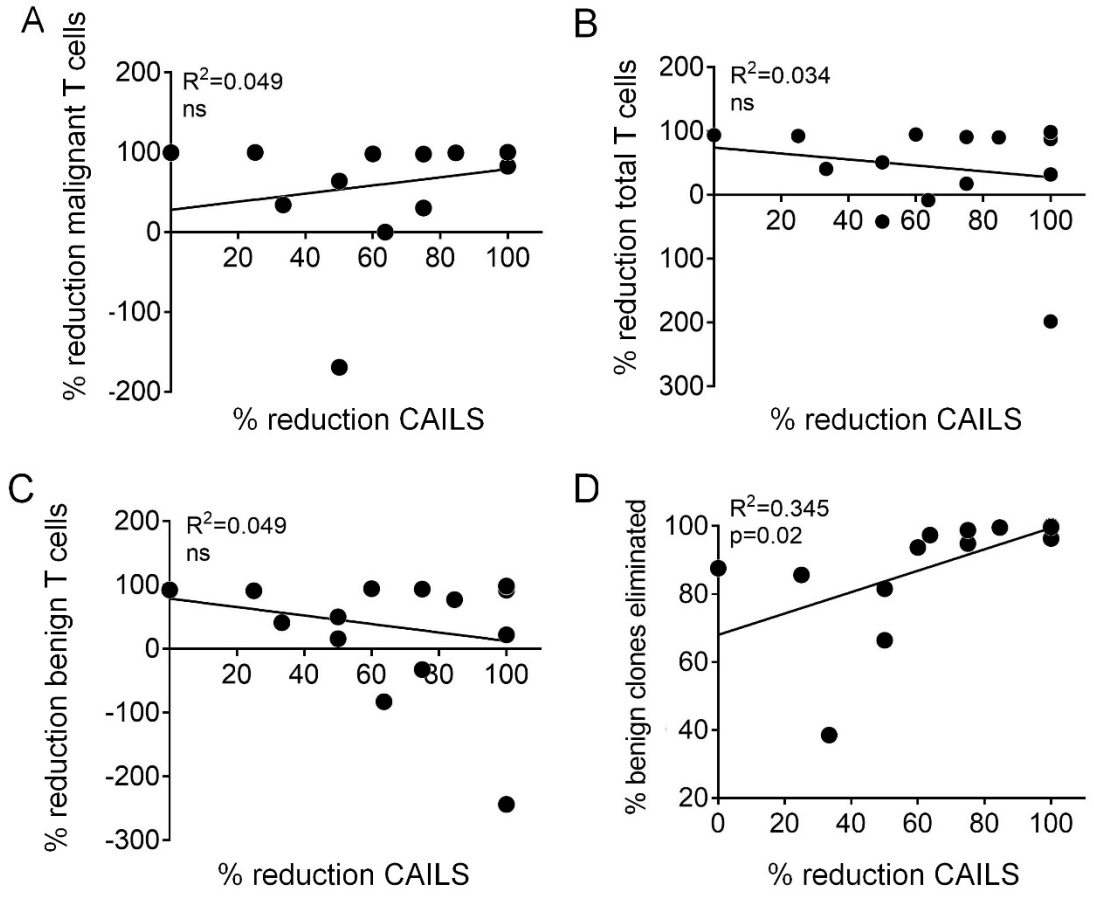

Fig. S1. Improvement in inflammation is correlated with shift in the benign T cell population but not with depletion of malignant T cells. Improvement in inflammation (CAILS) did not correlate with reductions in the number of malignant T cells **(A)**, total T cells **(B)** or benign T cells **(C)**. However, the loss of specific T cell clones from skin and recruitment of a second, distinct T cell population was correlated with reduced inflammation as assessed by CAILS scores (**D**).

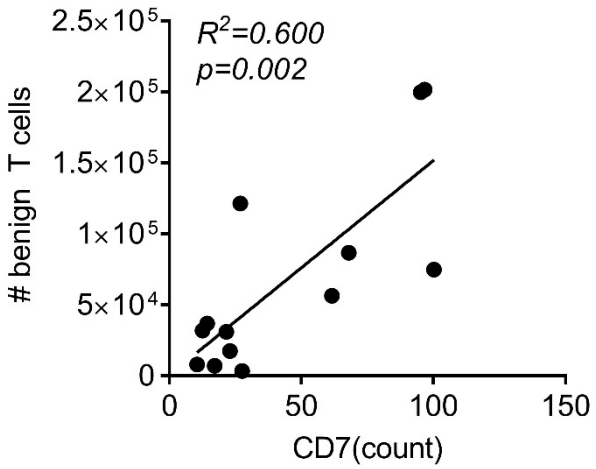

Fig. S2. CD7 gene counts correlate with the number of benign T cells as measured by HTS. The number of benign T cells per 100 ng of DNA as measured by HTS, correlates with gene expression of CD7 as measured by NanoString.

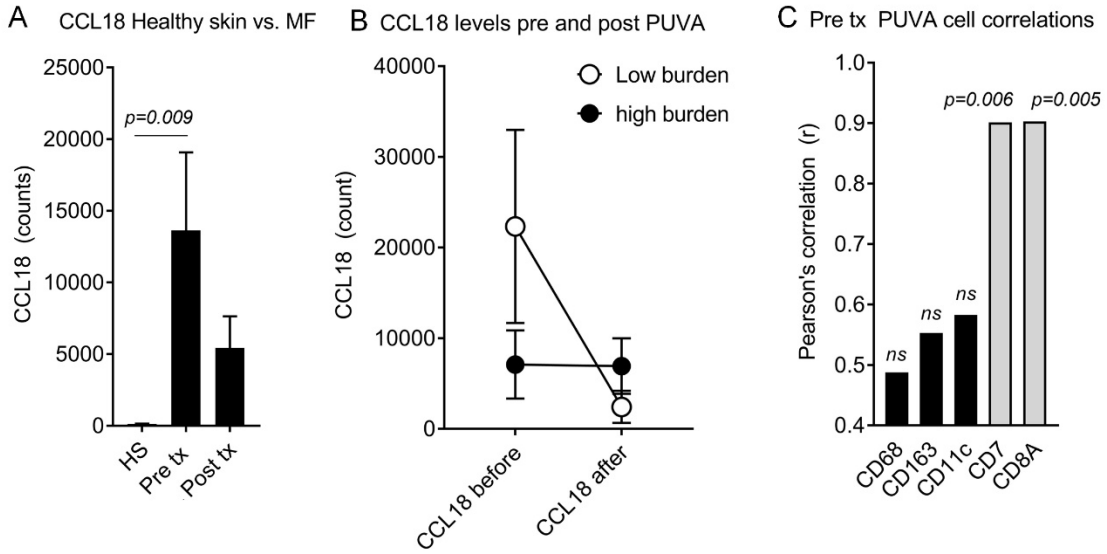

Fig. S3. CCL18 expression levels and cell associations. (A) CCL18 gene was expressed in pre-treatment MF (Pre tx) at levels 115-fold higher than in healthy skin (HS) and was reduced after PUVA therapy (Post tx). **(B)** CCL18 expression levels in low burden (less than 20% malignant T cells) and high burden (>20% malignant T cells) patients before (CCL18 before) and after (CCL18 after) PUVA therapy. **(C)** Genes associated with CCL18 before PUVA treatment.

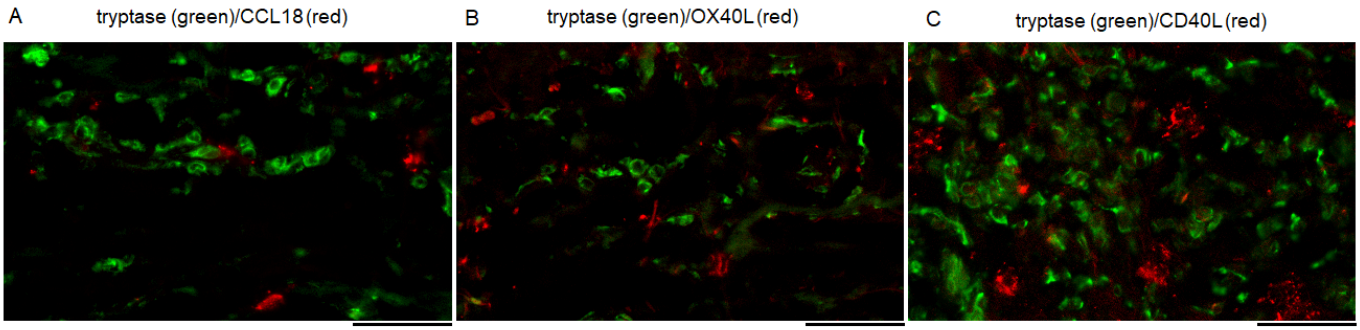

Fig. S4. Mast cells do not express CCL18, OX40L or CD40L. (A) Staining for the mast cell specific marker tryptase and CCL18 is shown for a patient with high burden Stage IB CTCL. A lack of co-staining indicates that CCL18 producing cells are not mast cells. **(B)** Tryptase and OX40L staining is shown for a patient with high burden Stage IB CTCL. **(C)** Tryptase and CD40 staining is shown for a patient with high burden Stage IIA MF. In all cases, CCL18, OX40L and CD40L did not co-localize. Similar results were observed in 3 MF patients. Scale bars, 100 μm.

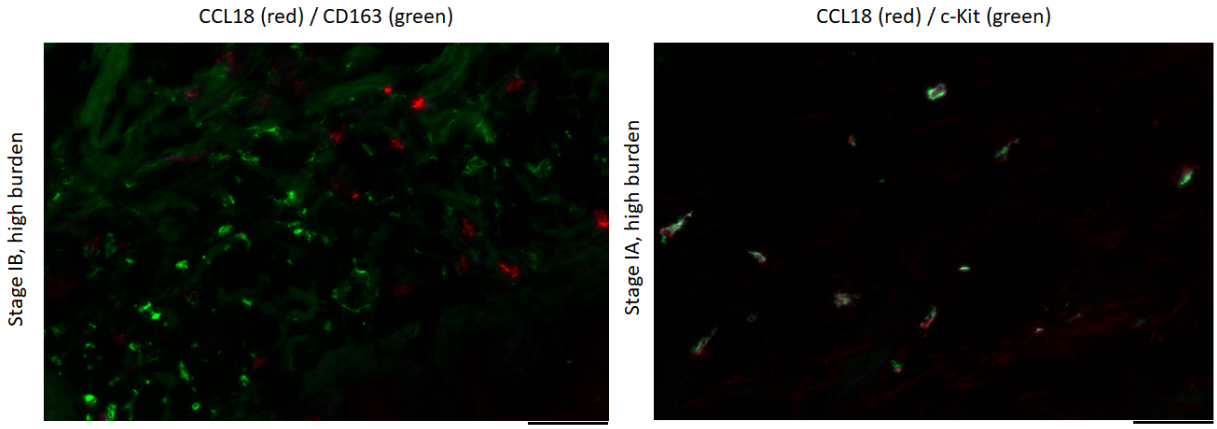

Fig. S5. Additional donors for observations shown in Fig. 4A (left panel) and Fig. 4B (right panel). Scale bars, 100 μm.

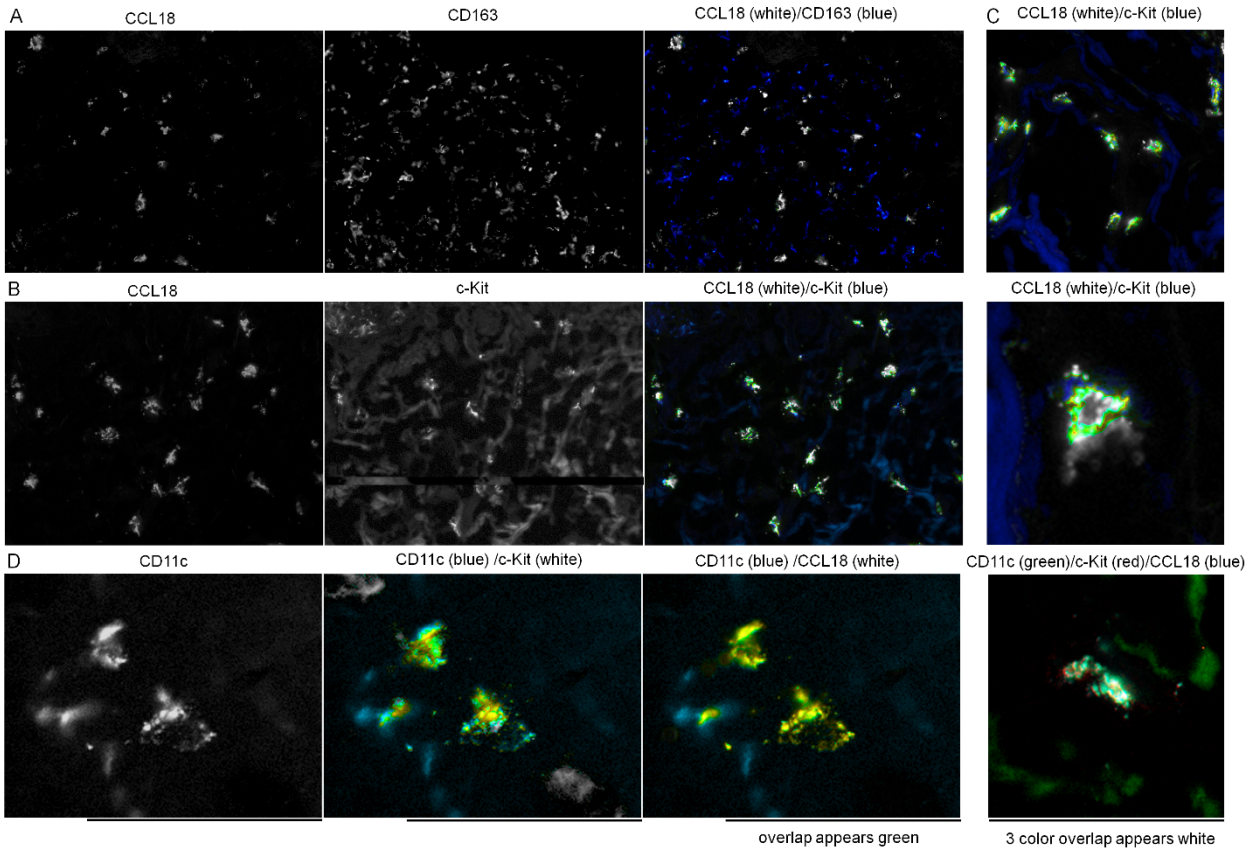

Fig. S6. Color blind accessible version of Figure 4. CCL18 is produced by c-Kit$^+$ dendritic cells in mycosis fungoides. (A) CD163 expressing M2-like macrophages do not produce CCL18 in MF. Co-immunostaining of CCL18 (monochrome white) and CD163 (blue) demonstrated independent staining. Areas of co-localization of the two stains appear green. A patient with low burden Stage IA CTCL is shown; a total of three Stage IA-IB patients showed similar results.; a total of three Stage IA-IB patients showed similar results. **(B-C)** CCL18 immunostaining colocalized with c-Kit expressing dermal cells. A Stage IB MF patient is shown; a total of four patients showed similar results. **(C)** Higher power images of immunostaining in the same Stage IA patient studied in **(A)** are shown. **(D)** CCL18 producing c-Kit$^+$ cells are CD11c$^+$ dendritic cells. A stage IA high burden patient is shown (first three panels) and co-staining for all markers in another Stage IB high burden patient is shown (fourth panel). Triple staining appears white. Stains demonstrating that CCL18$^+$ cells lacked expression of tryptase are included in Fig. S4. Similar results were observed in high and low burden patients. All lesions are untreated. Scale is same as for Fig. 4.

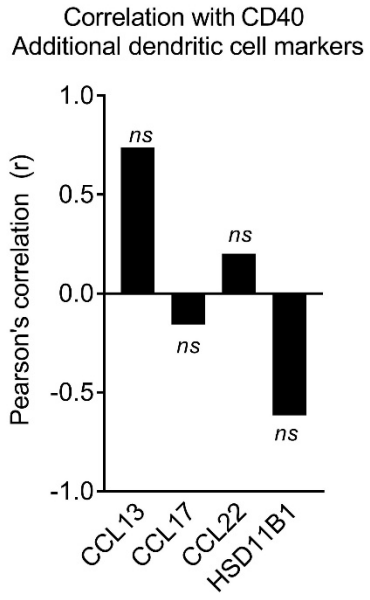

Fig. S7. Lack of correlation of CD40 with additional dendritic cell markers. Correlations are shown for CCL13, CCL17, CCL22 and HSD11B1. This data supplements CD40 correlations shown in Figure 5C.

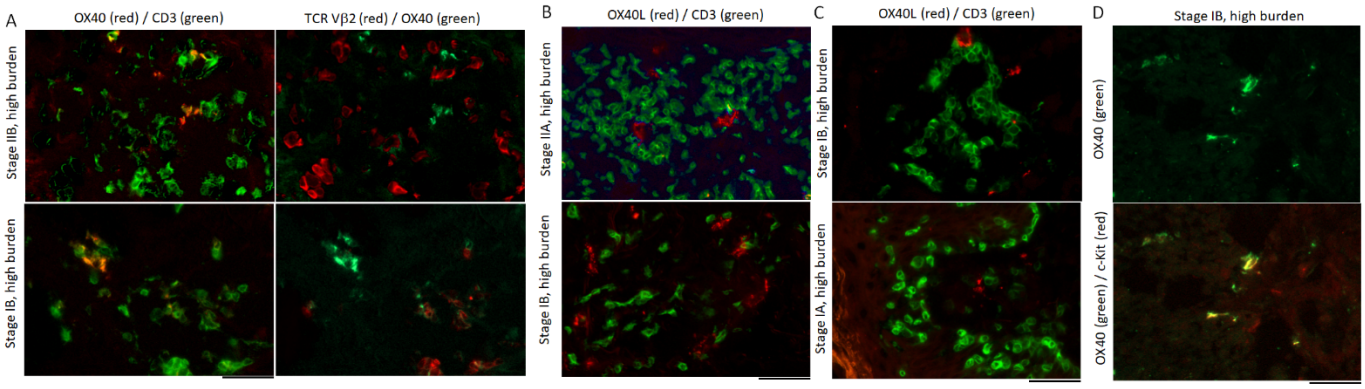

Fig. S8. Additional donors for observations shown in Fig. 6. (A) Replicate donors for observations reported in Fig. 6B,C. **(B)** Replicate donors for observations reported in Fig. 6D. **(C)** Replicate donors for observations reported in Fig. 6E. Scale bars, 100 μm.

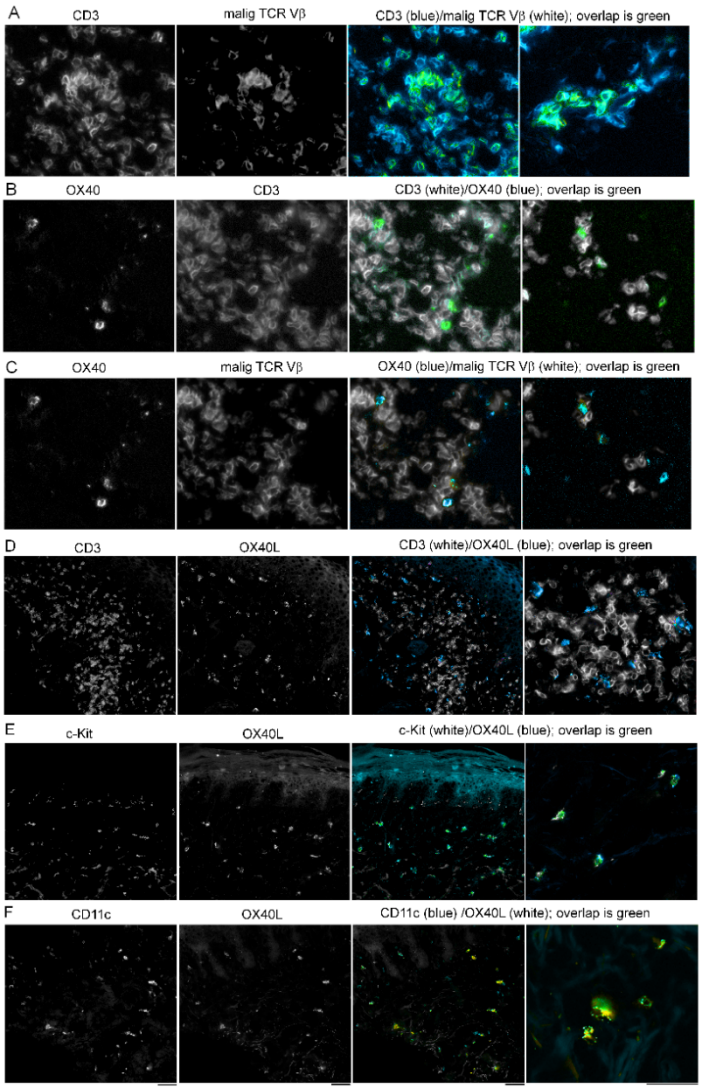

Fig. S9. Color blind accessible version of Figure 6. OX40 is expressed by benign T cells and OX40L is expressed by c-Kit$^+$ dendritic cells in mycosis fungoides. (A) Malignant and benign T cells can be discriminated by co-staining for CD3 and the TCR Vβ expressed by the malignant T cell clone, as identified by HTS. Malignant T cells co-stain for CD3 and the malignant T cell TCR Vβ (areas of co-localization of the two stains appear green) and benign T cells stain only for CD3 (blue). Stains of a patient with high burden Stage IIA are shown; A second field from the same donor is shown in the last panel. **(B)** OX40 is expressed by T cells in MF. A patient with high burden Stage IIA CTCL is shown. A second field from the same donor is shown in the last panel. Similar results were observed in a total of 3 donors. **(C)** OX40 is expressed by benign but not malignant T cells. OX40 and malignant T cell TCR Vβ antibodies stained distinct populations of T cells. A patient with high burden Stage IIA CTCL is shown. A second field from the same donor is shown in the last panel. Similar results were observed in a total of 3 donors. **(D)** OX40L is not expressed by T cells in MF. Antibodies specific for CD3 and OX40L stained distinct T cell populations. A patient with low burden Stage IA CTCL is shown; similar results were observed in a total of 5 donors. **(E)** OX40L is expressed by c-Kit$^+$ cells in MF. Stains of OX40L and c-Kit colocalized. A patient with high burden Stage IB CTCL is shown; similar results were observed in a total of three donors. **(F)** OX40L expressing cells are CD11c$^+$ dendritic cells. A patient with high burden Stage IA (first three panels) and a second patient with high burden Stage IB (fourth panel) MF are shown. Stains demonstrating that OX40L$^+$ cells lacked expression of tryptase are included in Fig. S4. All stains were performed on pre-treatment skin biopsies. Scale is same as for Fig. 6.

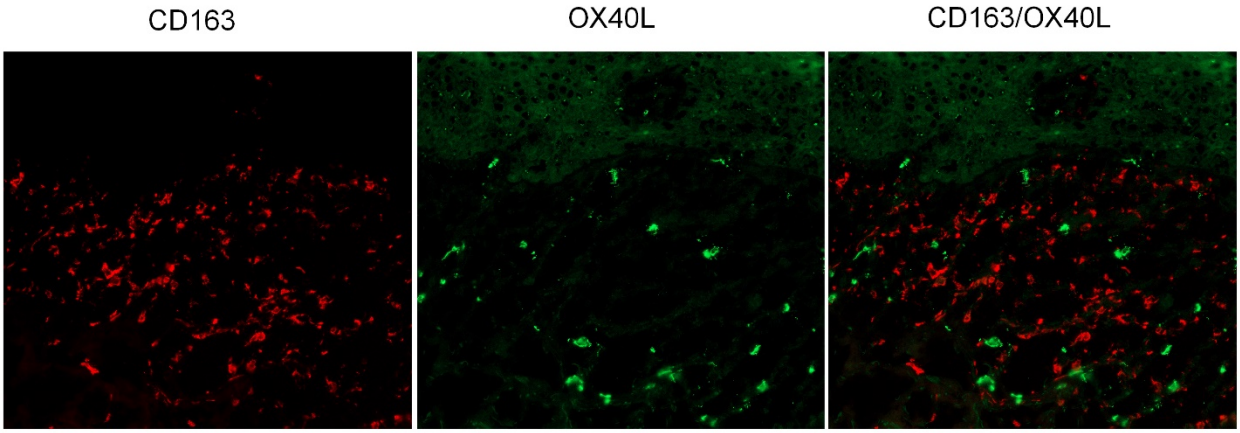

Fig. S10. OX40L was not expressed by CD163$^+$ macrophages in MF. Representative immunostaining of a patient with Stage IA CTCL is shown. Results were confirmed in a second patient with Stage IB MF.

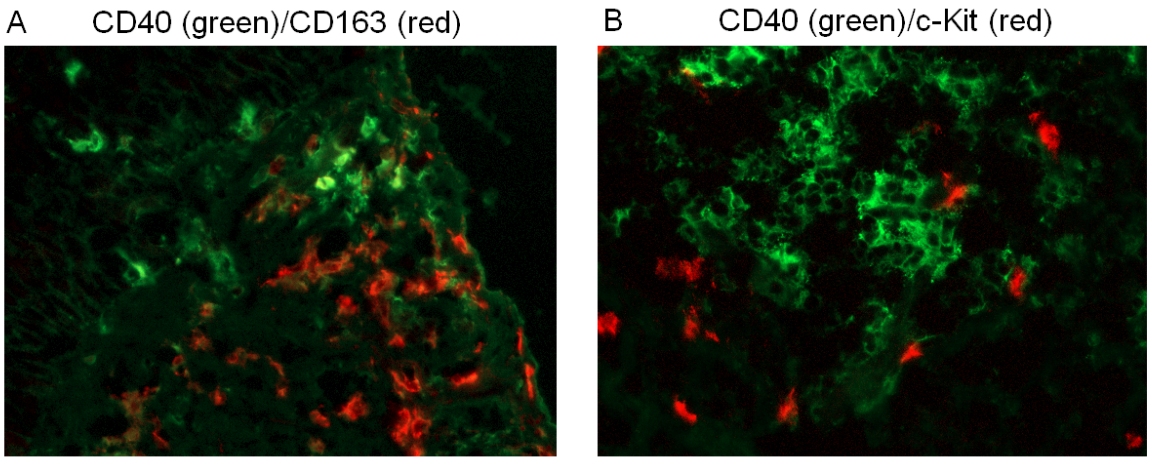

Fig. S11. CD40 was not expressed by (A) CD163$^+$ macrophages nor (B) c-Kit$^+$ cells in MF. Immunostains of patients with Stage IB (A) and IA (B) CTCL are shown. Similar results were observed in a total of three patients.

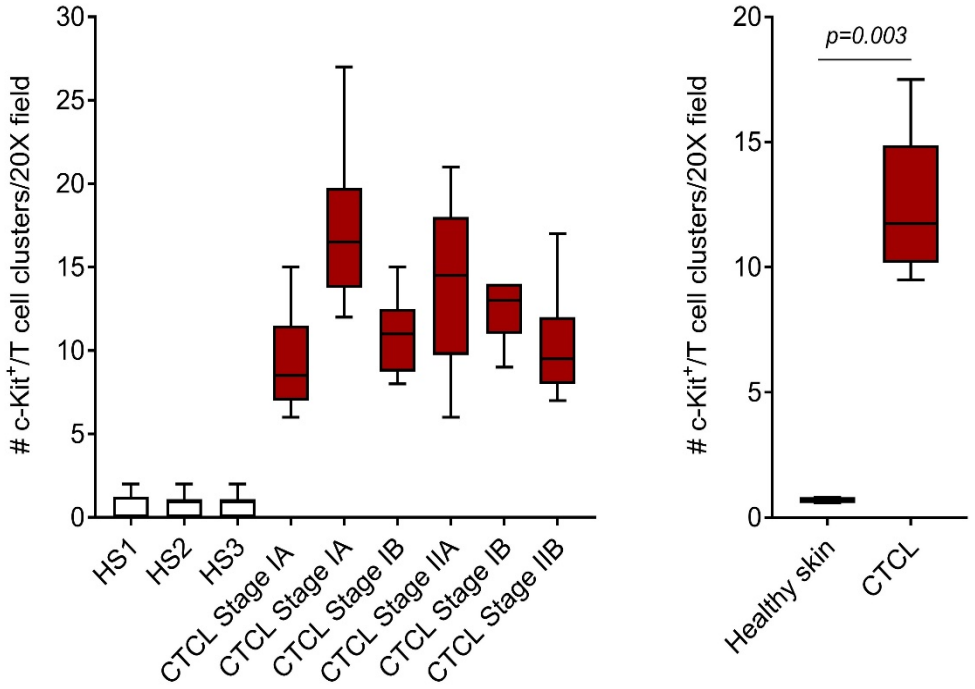

Fig. S12. C-Kit$^+$ DC-T cell aggregates are frequent in CTCL but rare in healthy skin. The number of c-Kit+ DC/T cell clusters per 20X field, defined as at least one T cell in contact with a c-Kit$^+$ cell, were quantified in three healthy skin donors (HS1-3) and six pre-treatment lesional CTCL skin biopsies. Statistics for individual patients (left panel) and aggregated healthy vs. disease (right panel) are shown. A minimum of five 20X fields were analyzed for each patient. The mean and range of the data are indicated. Differences between two sample groups were detected using the one tailed Wilcoxon–Mann–Whitney test, α=0.05.

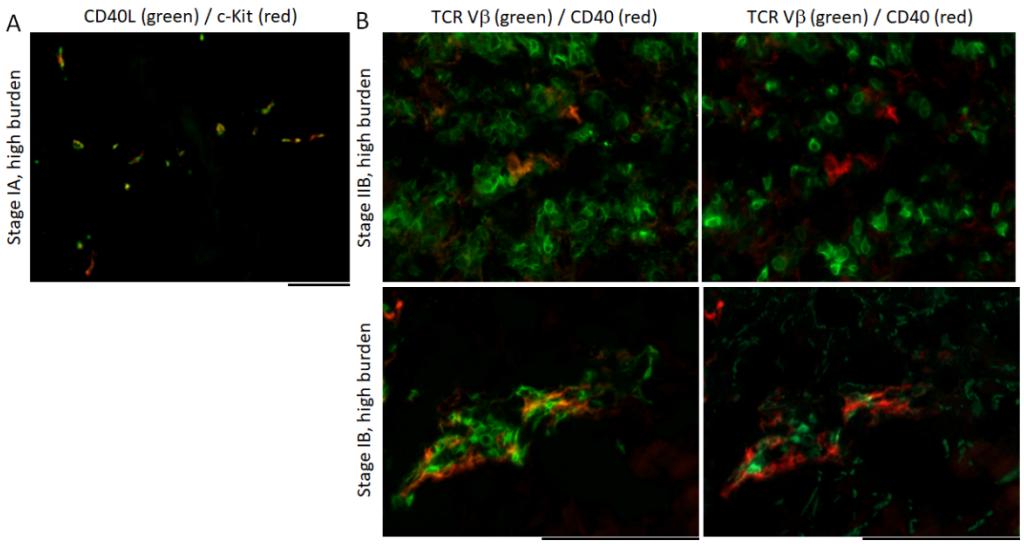

Fig. S13. Additional donors for observations shown in Fig. 7. (A) Additional donor for observation reported in Fig. 7B. **(B)** Replicate donors for observations reported in Fig. 7C. Scale bars, 100 μm.

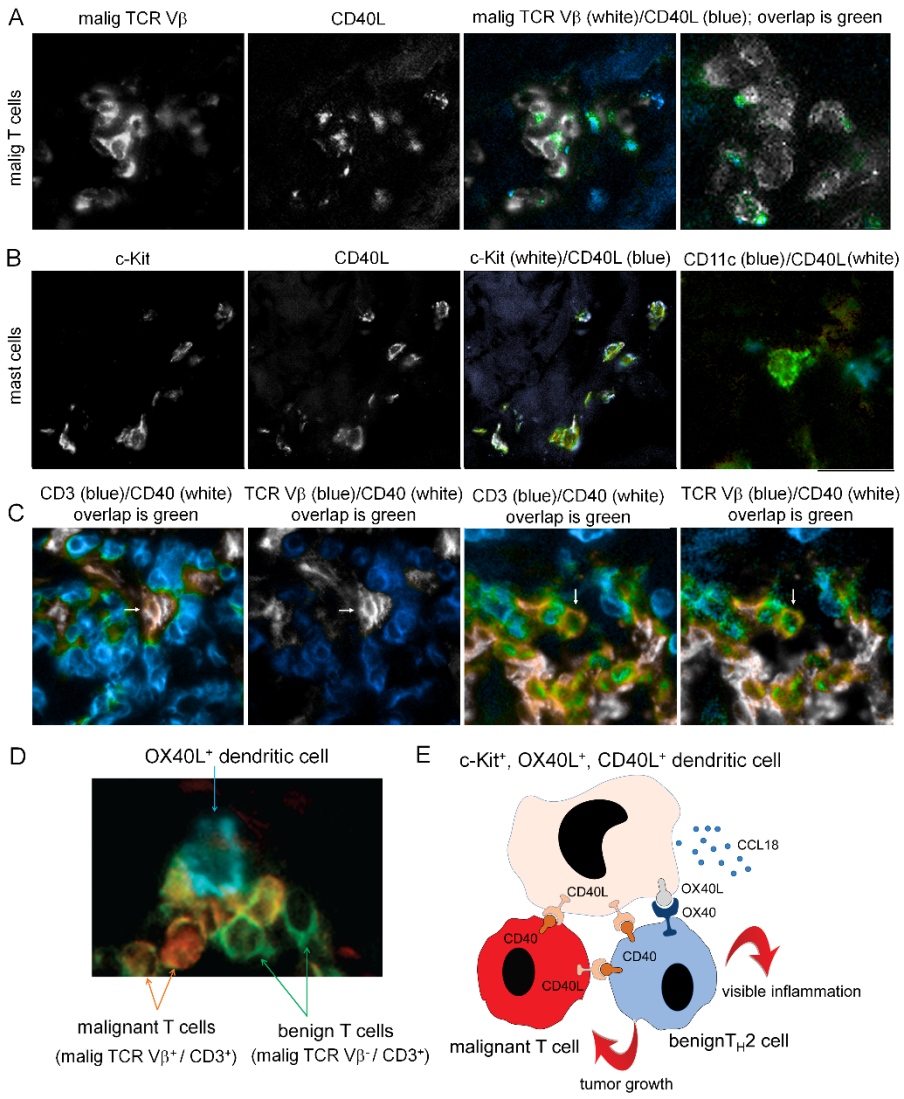

Fig. S14. Color blind accessible version of Figure 7. CD40/CD40L interactions may participate in an inflammatory synapse created between c-Kit$^+$ dendritic cells, malignant T cells and benign T cells in mycosis fungoides. **(A)** CD40L is expressed by malignant T cells. A patient with high burden Stage IIA (left three panels) and high burden stage IB (right panel) are shown. **(B)** CD40L is also expressed by c-Kit$^+$ dendritic cells. A patient with low burden Stage IA (left three panels) and high burden Stage IB (right panel) are shown; similar results were observed in a total of 3 donors. Co-staining of CD40L$^+$ cells with the DC marker CD11c is shown in the right panel. **(C)** Both benign and malignant T cells express CD40. The left two panels show benign T cells (CD3$^+$Vβ$^-$) T cells expressing CD40. The right two panels show malignant T cells (CD3$^+$Vβ$^+$) expressing CD40. Both fields are from the same high burden Stage IIA donor; similar results were observed in a total of three donors. **(D)** An inflammatory synapse is created between c-Kit$^+$ dendritic cells, malignant and benign T cells. Clusters of c-Kit$^+$ dendritic cells, benign and malignant T cells were frequently observed in MF, as illustrated by this co-stain for OX40L (c-Kit$^+$ dendritic cell) CD3 and the malignant TCR Vβ. Malignant and benign T cells are indicated by arrows instead of differentially pseudo-coloring this image. A patient with high burden Stage IIB is shown; clusters of these cells types were observed in five donors. **(E)** A proposed model for c-Kit$^+$ dendritic cell, benign and malignant T cell interactions in MF. Benign T cells are recruited by c-Kit$^+$ dendritic cell produced CCL18 and activated by OX40/OX40L and CD40/CD40L interactions leading to visible skin inflammation and pro-tumorogenic signals. C-Kit$^+$ dendritic cells may also directly stimulate malignant T cells via CD40/CD40L interactions. All stains were performed on pre-treatment skin biopsies. Scale is same as for Fig. 7.

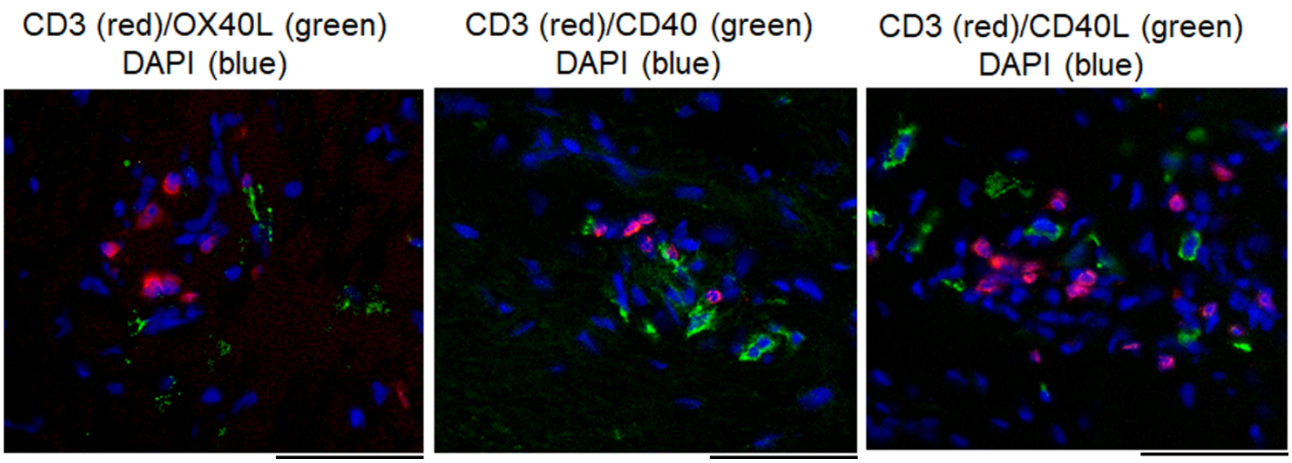

Fig. S15. T cells in healthy skin do not express CD40, CD40L or OX40L. Samples of healthy human skin are shown co-stained for CD3 and OX40L (left panel), CD40 (middle panel) and CD40L (right panel). A lack of co-staining demonstrates that these molecules are not expressed by T cells in healthy skin. Similar results were seen in three healthy skin donors.

Table S1. Genes associated with CD7 before and after PUVA therapy.

Pre-PUVA CD7 associated genes			Post-PUVA CD7 associated genes		
Gene	**r**	**P (two-tailed)**	**Gene**	**r**	**P (two-tailed)**
EWSR1	0.978	0.0001	LTA	0.996	<0.0001
TNFRSF4	0.971	0.0003	NFKB1	0.996	<0.0001
NEFL	0.916	0.0037	S100A12	0.995	<0.0001
CD274	0.915	0.0038	CXCL9	0.994	<0.0001
CSF1	0.910	0.0044	CXCL11	0.994	<0.0001
CCL18	0.901	0.0056	CD79B	0.994	<0.0001
PMCH	0.893	0.0067	LTB	0.992	<0.0001
CD8A	0.892	0.0069	ISG20	0.990	0.0001
GZMM	0.889	0.0074	NFATC1	0.990	0.0002
CD80	0.881	0.0089	IL22RA2	0.989	0.0002
CXCL16	0.876	0.0097	IFNAR2	0.989	0.0002
			IDO1	0.987	0.0002
			CD19	0.987	0.0003
			TRAF2	0.987	0.0003
			TLR10	0.987	0.0003
			NFKBIA	0.986	0.0003
			MS4A1	0.984	0.0004
			CD22	0.983	0.0004
			PAX5	0.982	0.0005
			SH2D1B	0.981	0.0005
			VCAM1	0.981	0.0005
			LRRN3	0.980	0.0006
			KLRB1	0.980	0.0006
			CXCL13	0.979	0.0006
			ISG15	0.979	0.0007

			EBI3	0.979	0.0007
			NCAM1	0.979	0.0007
			CXCR5	0.977	0.0008
			IL2RA	0.977	0.0008
			BLK	0.976	0.0009
			CD8B	0.975	0.001
			CD40LG	0.973	0.0011
			ADORA2A	0.972	0.0012
			CR2	0.970	0.0013
			MX1	0.970	0.0013
			ICOS	0.969	0.0014
			FCER2	0.969	0.0014
			TLR9	0.968	0.0015
			GZMB	0.965	0.0018
			CYLD	0.964	0.0019
			IFIH1	0.964	0.0019
			CCL4	0.962	0.0022
			DUSP4	0.961	0.0023
			NFKB2	0.960	0.0024
			SIGIRR	0.959	0.0025
			CD207	0.959	0.0025
			LAIR2	0.957	0.0027
			ATG12	0.956	0.0028
			IRF7	0.956	0.0028
			LILRB1	0.955	0.003
			IL2RG	0.953	0.0033
			KLRC1	0.953	0.0033
			CCND3	0.952	0.0035

			CXCL10	0.951	0.0035
			TNFRSF13C	0.951	0.0035
			CHIT1	0.951	0.0036
			POU2F2	0.948	0.0039
			JAK3	0.948	0.004
			DDX58	0.946	0.0042
			BTLA	0.946	0.0042
			CCL5	0.945	0.0045
			CSF2RB	0.943	0.0048
			CD83	0.942	0.0049
			KLRD1	0.941	0.0051
			IL6	0.939	0.0056
			IL19	0.938	0.0057
			CSF3	0.935	0.0062
			GZMM	0.935	0.0063
			TNF	0.934	0.0063
			CCR9	0.934	0.0065
			IL16	0.931	0.0069
			CXCR4	0.928	0.0076
			LILRA4	0.927	0.0077
			PDCD1	0.926	0.008
			RUNX3	0.926	0.0081
			SLAMF1	0.926	0.0081
			CCL3L1	0.925	0.0082
			RELB	0.924	0.0084
			CD37	0.924	0.0086
			CD47	0.923	0.0087
			CCL15	0.922	0.0088

			ITGA4	0.922	0.009
			TNFSF14	0.921	0.0091
			CD6	0.920	0.0094
			CLU	0.917	0.01

*Genes with $r \geq 0.8$ and $p \leq 0.01$ are listed.

Table S2. Genes associated with CD8A before and after PUVA therapy.

Pre-PUVA CD8 associated genes			Post-PUVA CD8 associated genes		
Gene	**r**	**P (two-tailed)**	**Gene**	**r**	**P (two-tailed)**
CD274	0.987	<0.0001	KLRK1	0.992	<0.0001
CD80	0.988	<0.0001	GZMK	0.991	0.0001
SEMG1	0.970	0.0003	CD5	0.985	0.0003
CTAGE1	0.966	0.0004	CD3E	0.984	0.0004
IGF2R	0.967	0.0004	LCK	0.979	0.0007
CXCR1	0.945	0.0013	CD3D	0.977	0.0008
PMCH	0.946	0.0013	CD6	0.970	0.0013
CXCL16	0.939	0.0017	CXCR4	0.970	0.0013
MICA	0.924	0.0029	CD3G	0.970	0.0014
NOD1	0.915	0.0039	RUNX3	0.967	0.0016
GZMM	0.912	0.0042	TNFSF14	0.966	0.0017
CCL18	0.903	0.0053	ICAM3	0.965	0.0018
ITGAM	0.903	0.0053	IL2RG	0.964	0.0019
IFNA8	0.903	0.0054	NUP107	0.961	0.0023
TIRAP	0.903	0.0054	PTPRC	0.957	0.0027
SPO11	0.897	0.0061	CYFIP2	0.957	0.0028
TNFRSF4	0.895	0.0065	SIGIRR	0.957	0.0028
CD7	0.892	0.0069	CCL4	0.951	0.0036
TMEFF2	0.891	0.0072	CD2	0.950	0.0037
CCL2	0.889	0.0075	CD247	0.949	0.0039
TREM2	0.885	0.0082	NFKB2	0.948	0.004
EWSR1	0.884	0.0083	TANK	0.947	0.0041
PLAU	0.880	0.009	ICAM2	0.947	0.0042

IRF5	0.878	0.0094	CCND3	0.946	0.0044
			CCR4	0.945	0.0044
			CARD11	0.944	0.0046
			TLK2	0.942	0.0049
			CCL5	0.941	0.0052
			LY9	0.938	0.0057
			SPN	0.937	0.0058
			CD79A	0.937	0.0059
			TNFSF15	0.934	0.0064
			CD200	0.931	0.007
			CCR9	0.930	0.0071
			IL16	0.930	0.0071
			TNFRSF1B	0.930	0.0072
			POU2F2	0.928	0.0076
			PRPF38A	0.928	0.0076
			IL21R	0.927	0.0078
			PIK3CD	0.924	0.0084
			BTLA	0.923	0.0087
			CD27	0.922	0.0088
			IL6R	0.923	0.0088
			JAK3	0.922	0.0089
			IFI16	0.921	0.0092
			TNF	0.920	0.0093

*Genes with $r \geq 0.8$ and $p \leq 0.01$ are listed.

Table S3. Genes associated with the number of malignant T cells/100 ng DNA before and after PUVA therapy.

Pre-PUVA Malignant			Post-PUVA malignant		
Gene	**r**	**P (two-tailed)**	**Gene**	**r**	**P (two-tailed)**
TNFSF4	0.959	0.0006	BCL10	0.9761	0.0009
BTLA	0.940	0.0016	KIR3DL1	0.9703	0.0013
CD40LG	0.932	0.0022	ATF1	0.9691	0.0014
ITK	0.933	0.0022	MAPKAPK2	0.966	0.0017
ETS1	0.927	0.0027	TNFRSF13B	0.9543	0.0031
CXCR4	0.907	0.0048	CTSH	0.9522	0.0034
CCND3	0.902	0.0055	CD38	0.9509	0.0036
NCAM1	0.902	0.0055	HLA-C	0.9349	0.0062
CD3G	0.884	0.0083	POU2AF1	0.935	0.0062
NUP107	0.880	0.009	LY86	0.9317	0.0068
RUNX3	0.878	0.0093	SH2B2	0.9296	0.0073
SIGIRR	0.876	0.0097			

*Genes with $r \geq 0.8$ and $p \leq 0.01$ are listed.

Table S4: Antibodies used in these studies

Antibody	Fluorophore	Clone	Company	Catalog #	Concentration
CCL18	AlexaFluor 594	64507	R&D Systems	IC394T-100UG	1:15
CD163	AlexaFluor 488	215927	R&D Systems	FAB1607G-100	1:7.5
Ckit	AlexaFluor 647	104D2	Biolegend	313236	1:5
Ckit	FITC	104D2	Biolegend	313232	1:5
Vbeta 2	PE	MPB2D5	Beckman Coulter	IM2213	1:10
Vbeta 5.1	PE	IMMU 157	Beckman Coulter	IM2285	1:10
CD3	AlexaFluor 647	UCHT1	Biolegend	300416	1:40
OX40	AlexaFluor 488	Ber-ACT35	Biolegend	Custom mAb	1:400
OX40L	AlexaFluor 594	159403	R&D Systems	FAB10541T-100UG	1:10
CD40	unconjugated	5C3	Abcam	ab134379	1:500
CD40L	AlexaFluor 594	40804	R&D Systems	FAB617T-100UG	1:25
CD11c	AlexaFluor 488	ICRF 3.9	R&D	FAB1777G-100UG	1:50
Tryptase	unconjugated	Polyclonal	Abcam	ab196772	1:500
Goat anti-rabbit 2˚	AlexaFluor 594		Life Tech	A11012	1:1000
Goat anti-rabbit 2˚	AlexaFluor 647		Life Tech	A21224	1:1000
Rabbit anti-mouse 2˚	AlexaFluor 594		Life Tech	A11062	1:1000
Rabbit anti-mouse 2˚	AlexaFluor 488		Life Tech	A11054	1:1000